This document is the accepted manuscript version of the following article: Devlioglu, A., Vockenhuber, M., Van Lent-Protasova, L., Mochi, I., Ekinci, Y., & Kazazis, D. (2023). Advancements in EUV photoresists for high-NA lithography. In P. P. Naulleau, P. A. Gargini, T. Itani, & K. G. Ronse (Eds.), Proceedings of SPIE - the international society for optical engineering: Vol. 12750. International conference on extreme ultraviolet lithography (p. 1275008 (11 pp.). https://doi.org/10.1117/12.2686250

Advancements in EUV photoresists for high-NA lithography

Aysegul Devlioglu[a], Michaela Vockenhuber[a], Lidia van Lent-Protasova[b], Iacopo Mochi[a], Yasin Ekinci[a], Dimitrios Kazazis[a]
[a] Paul Scherrer Institut, 5232, Villigen-PSI, Switzerland
[b]ASML, De Run 6501, 5504 DR Veldhoven, The Netherlands

ABSTRACT

EUV resist materials play a vital role in enabling advanced lithographic technologies for high-volume manufacturing (HVM) targeting nodes below 5 nm. In this study, we report an extensive performance characterization of available EUV photoresists for future high-NA EUV lithography. We investigated the performance of various resists using the EUV interference lithography tool at the Swiss Light Source (SLS) within the framework of a collaboration between the Paul Scherrer Institute and ASML. This paper highlights the major improvements we observed in 2023 and presents the best performing resists of 6 different vendors for half-pitch (HP) 14 and below. Important performance characteristics considered in this study are resolution or HP, dose-to-size (DtS) and line-width roughness (LWR). To evaluate the overall performance of the resists, we used the Z-factor. We investigated both chemically amplified resists (CAR) and non-CAR materials. CARs from two vendors achieved a resolution down to 11 nm half-pitch, while multi-trigger resists (MTR) reached a resolution of 13 nm. A new metal organic resist (MOR) achieved a resolution down to 11 nm. MTR and one CAR material achieved the lowest Z-factor to date. In addition, we investigated the effect of underlayers on the performance of MOR and compared the performance of the new MOR to the predecessor. We, finally, discuss the overall progress in resist performance over the recent years. We observed a steady improvement across several resist platforms, which is encouraging for global EUV resist development towards high-NA EUVL.

Keywords: EUVL, Photoresist, High-NA, Interference Lithography

INTRODUCTION

Extreme ultraviolet (EUV) lithography entered high volume manufacturing (HVM) in 2019 to enable further miniaturization of semiconductor devices, following the Moore's Law[1]. To keep up with the scaling trend in the coming decades, EUV lithography with higher resolution is needed and therefore high-NA scanners are being developed and expected to enter HVM in 2025. High-NA patterning will require the use of photoresists beyond what is available in HVM today towards single digit nanometer patterning. To this end, the Paul Scherrer Institute (PSI) and ASML have partnered in a longstanding collaboration to support the photoresist community in the development of suitable materials (resists and underlayers) for both the current 0.33 NA tools and for the future high-NA nodes[2-4]. In the framework of this collaboration, we have supported academic and industrial groups to develop, test, and evaluate the performance of their materials.

PSI operates several large-scale facilities, among which is the Swiss light source (SLS). The XIL-II is a SLS beamline optimized for EUV wavelength and is dedicated to EUV metrology and lithography. The lithography experiments take place at an interferometric setup located inside a cleanroom. The patterned photoresists are characterized with ultrahigh resolution scanning electron microscopy (SEM) following a protocol based to a large extent on the IMEC roughness protocol[5] and the image analysis is performed with the SMILE software[6] to extract the resist performance metrics.

In 2023, we investigated more than 100 resist materials for existing NXE and future high-NA scanners. Here, we report the performance of the best resists of five different providers for 14 nm half-pitch (HP) and below. We also outline the progress made in resists during the past three years.

EUV interference lithography

Our exposure method for the resist evaluation is based on EUV interference lithography (EUV-IL). For the resist evaluation we use a central wavelength of 13.5 nm with a bandwidth of about 4%. The XIL beamline and our EUV-IL technique have been previously described elsewhere in detail.[7] Briefly, EUV light is diffracted by two or more identical transmission gratings on a thin silicon nitride membrane[8] and the mutually coherent diffracted beams interfere, creating a periodic aerial image. In our work, we have used masks with two gratings which create high-resolution line/space (L/S) patterns. Because we use first-order diffraction beams, we benefit form a frequency multiplication effect thanks to which the pitch of the aerial image used to expose the resist is half the pitch of the gratings on the mask.[9] Besides high resolution due to frequency multiplication, the technique has also pitch- and focus-independent contrast.[10-11] The EUV-IL setup has a record resolution of 6nm HP[12] and it has been extensively used in photoresist development over the years due to its availability to both academic and industrial users, its simplicity, and tolerance to outgassing (as it has no expensive projection optics).

Experimental procedure

The materials to be tested are processed, exposed, and developed in a cleanroom environment at the XIL-II beamline. They are subsequently inspected using a high-resolution SEM (Hitachi Regulus 8230). The SEM parameters are in line with IMEC's roughness protocol to the extent that this is possible, considering that we employ an analytical SEM rather than a CD-SEM. We use a measured specimen current of 8 pA, a landing voltage of 500V, a pixel size of 0.83 nm and acquire the images with a charge suppression mode, trying to minimize the electron beam damage to the resist. As mentioned in the introduction, the image analysis is performed with the open-source software SMILE, developed in house at PSI.[6] Among the important metrics that we obtain through SMILE are the average critical dimension (CD), the local CD uniformity (LCDU), and the unbiased linewidth roughness (LWR). The results are then analyzed as a function of exposure dose to extract the dose-to-size (DtS). From the CD, LWR, and DtS we also calculate the Z-factor[13], as an overall resist performance metric. We note that the reported photon dose that reaches the resist at the wafer level has been cross calibrated with other tools.[4]

Program goals

The main target of the program is to characterize and optimize resist materials for the actual 0.33 NA systems with sub-13 nm resolution as well as to support the industry and boost the resist development towards high-NA with resolutions down to 8 nm HP. Table 1 shows the general guidelines targeted in the resist screening program.

Table 1: General guidelines targeted in the resist screening program.

Features	L/S: 16 nm > CD > 8 nm
Resist type	CAR, non-CAR
Resist thickness	20 – 30 nm
Throughput	DtS < 60 mJ/cm^2
Roughness	LWR< 10%
General performance	Z-factor = CD^3·LWR^2·DtS

RESULTS

In this section, we present the best-performing resists of each type from HP 14 nm to higher resolutions. We present the three positive-tone CAR, one negative-tone MTR and one MOR. Figure 1 shows SEM images of the one of the best performing CARs from HP 14 to 10 nm. Vendor A – CAR has well defined, well resolved and defect free lines at HP 14 and HP 13. It has minor bridging at HP 12 nm and almost resolves down to HP 11. However, at HP 11 some broken lines start to appear while HP 10 nm is not resolved.

Table 2 shows the performance metrics of the resists shown in Figure 1. This resist meets the DtS requirement at all pitches, as shown in Table 1. However, LWR and Z-factor values are above the program target for all pitches.

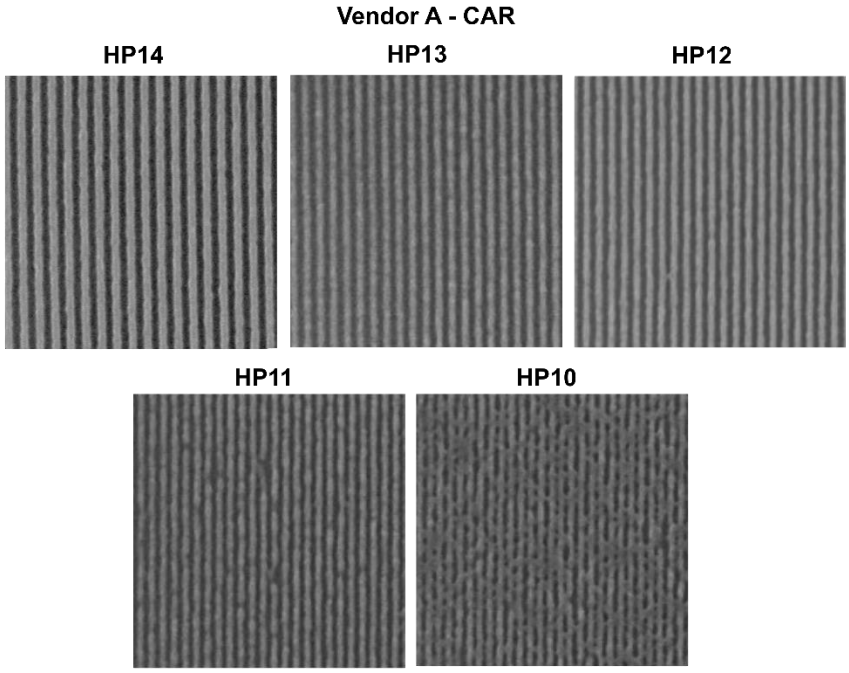

Figure 1. SEM images of Vendor A - CAR from HP 14 nm to HP 10 nm.

Table 2. Performance metrics of Vendor A – CAR from HP 14 nm to HP 12.

Vendor A - CAR	HP 14 nm	HP 13 nm	HP 12 nm
DtS (mJ/cm^2)	38.1	38.4	42.2
LWR (nm)	2.64	2.64	2.81
Z-factor (x10^{-8}) (mJ·nm^3)	0.73	0.59	0.57

Figure 2 shows the SEM images of Vendor B – CAR from HP 14 nm to 10 nm. This resist also has well defined lines with the resolution limit of HP 12 nm. The lines are fully resolved at HP 12 nm, and they start to show defects (bridging and broken lines) at HP 11 nm and HP 10 nm lines are not resolved.

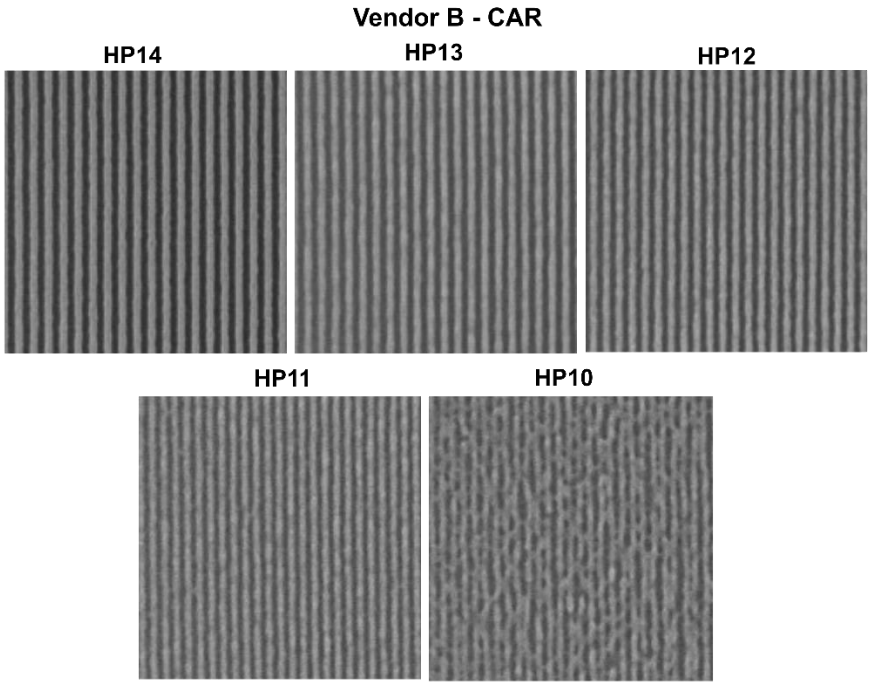

Figure 2. SEM images of Vendor B – CAR from HP 14 nm to HP 10 nm.

Table 3 shows the performance metrics of the resist from Figure 2. This resist requires more dose compared to CAR A and does not meet the general guidelines for HP 14 nm. However, it has lower roughness for HP 14 and 13. HP 13 nm and HP 12 nm meet the DtS criteria. Again, the corresponding LWR is above target for all pitches.

Table 3. Performance metrics of Vendor B – CAR from HP 14 nm to HP 12.

Vendor B - CAR	HP 14 nm	HP 13 nm	HP 12 nm
DtS (mJ/cm^2)	65.34	52.8	55.8
LWR (nm)	2.12	1.90	2.95
Z-factor ($x10^{-8}$) ($mJ \cdot nm^3$)	0.80	0.42	0.84

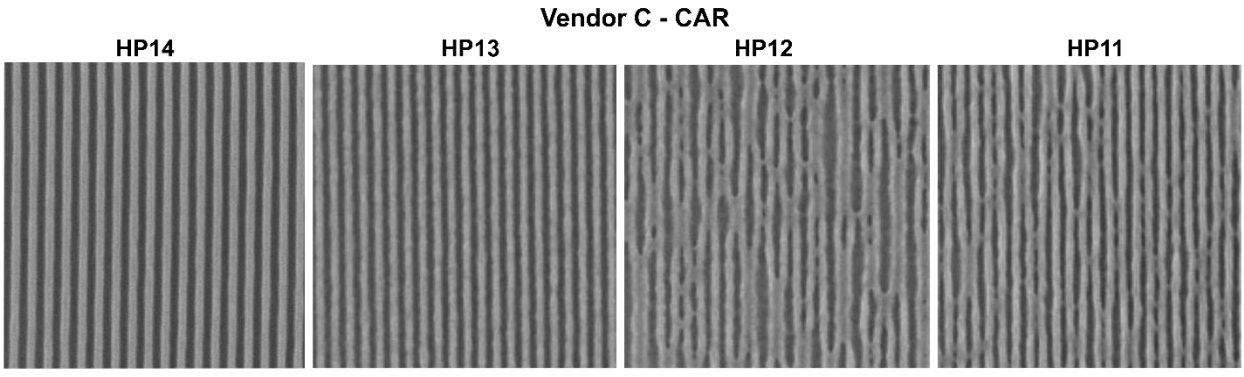

Figure 3. SEM images of Vendor C – CAR from HP 14 nm to HP 11 nm.

Figure 3 shows the SEM images of Vendor C from HP 14 nm to HP 11 nm. This resist has a resolution limit of 13 nm and suffers from pattern collapse at smaller pitches. The performance metrics of this resist are summarized in Table 4. Although this resist has lower resolution due to collapsed lines, it has significantly lower DtS and LWR compared to the previous CARs. HP 14 nm LWR is very close to the 10% target, and it has the lowest Z-factor achieved for CARs within this program.

Table 4. Performance metrics of Vendor C – CAR from HP 14 nm and HP 13.

Vendor C - CAR	**HP 14 nm**	**HP 13 nm**
DtS (mJ/cm^2)	36.70	26.0
LWR (nm)	1.50	2.88
Z-factor (x10^{-8}) (mJ·nm^3)	0.22	0.47

We now turn to a different resist category, namely the multi-trigger resists. The results of the best performing MTR are shown in Figure 4 from HP 14 nm to 10 nm, while Table 5 summarizes its performance metrics. This MTR has a resolution limit at 13 nm with a very low DtS that is within the requirement. The lines at HP 12 nm are also resolved but with multiple defects, while HP 11nm is not resolved. The measured LWR values are above the program specifications.

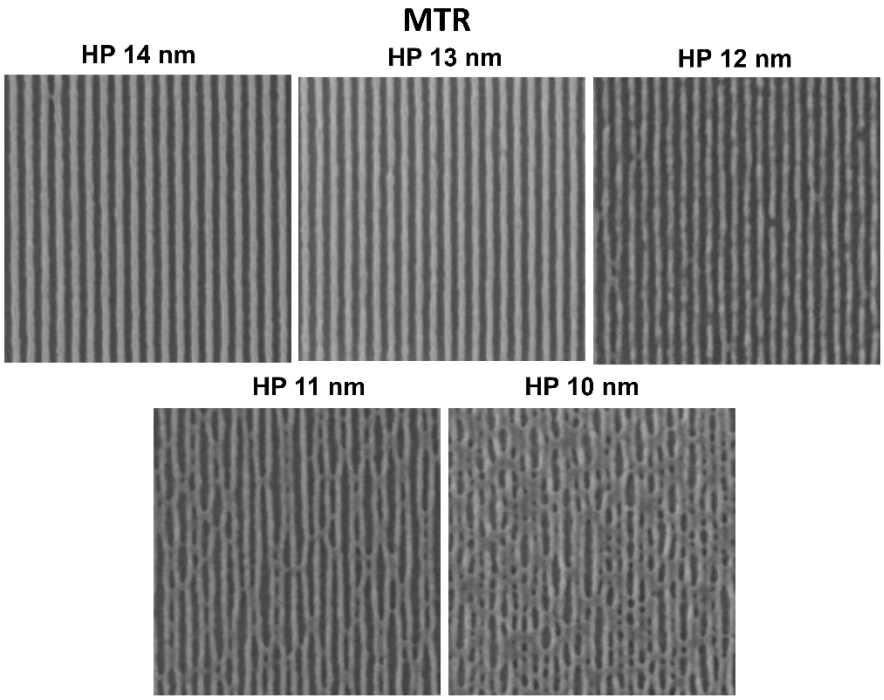

Figure 4. SEM images of the MTR from HP 14 nm to HP 10 nm.

Table 5. Performance metrics of the best performing MTR.

MTR	HP 14 nm	HP 13 nm
DtS (mJ/cm^2)	21.9	13.6
LWR (nm)	2.53	2.73
Z-factor (x10^{-8}) (mJ·nm^3)	0.38	0.22

As far as MOR are considered, Figure 5 shows the SEM images of the best resist from HP 14 nm to HP 10 nm. MOR has the best performance in terms of resolution with well-resolved lines at HP 11 nm. We note that in the case of the MOR, it was not the resist itself that was optimized but the underlayer material, which will be discussed further on. Table 6 shows the performance metrics of this resist. It is clear that, in terms of resolution, this resist outperforms the other resists, but in terms of the other requirements it is not performing as good. It is important to note that unavoidable delay between exposure and bake/development affects the quality of the lines for MOR.

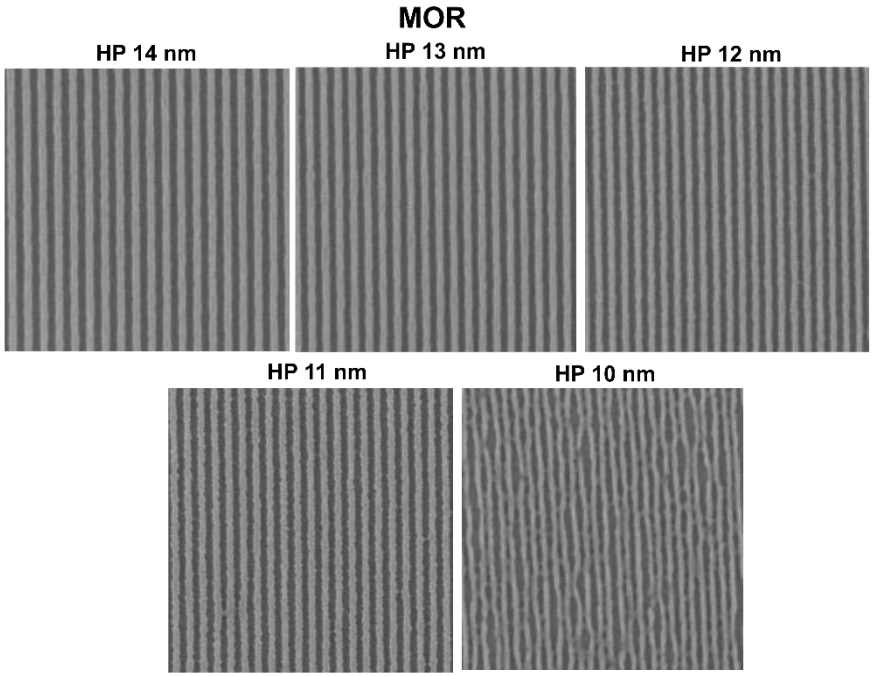

Figure 5. SEM images of the MOR from HP 14 nm to HP 10 nm.

Table 6. Performance metrics of MOR.

Metal organic resist	HP 14 nm	HP 13 nm	HP 12 nm	HP 11 nm
DtS (mJ/cm^2)	57.5	65.1	56.6	52.2
LWR (nm)	2.42	2.52	3.12	3.08
Z-factor (x10^{-8}) (mJ·nm^3)	0.92	0.78	0.95	0.66

Figure 6 shows the LWR plotted versus the exposure dose at HP 14 and 13 nm for the best performing resists of 5 vendors. The dashed line represents the iso-Z-factor line for the respective HP. Below these lines the resist performance for HP 14 nm and HP 13 nm lies within the program requirements. The iso-Z-factor lines are calculated with the DtS requirement of 60 mJ/cm^2, with LWR at 10% of the HP and with CD equal to HP. This gives the constant

Z-factors of 0.32×10^{-8} mJ·nm^3 for HP 14 nm and 0.22×10^{-8} mJ·nm^3 for HP 13 nm. The filled circles indicate a 1:1 ratio of lines to spaces for each resist. For HP 14 nm, the Vendor C - CAR and Vendor D - MTR and for HP 13 nm, only the MTR is within the iso-Z-factor line. Given that the general guideline for DtS is under 60 mJ/cm^2 and the requirement for the LWR is 10% of the CD, in stricter terms the resists should lie within the designated area in the plots.

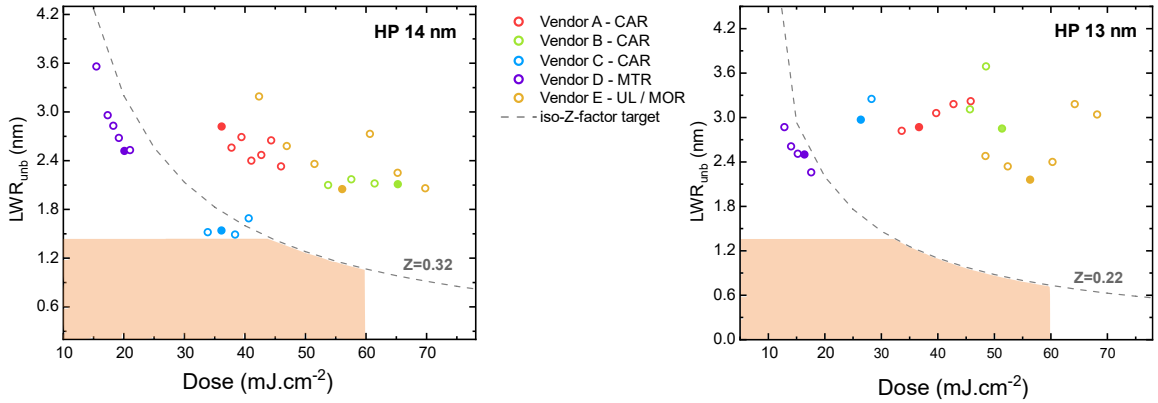

Figure 6. LWR as a function of dose for the best performing resists that were evaluated at (left) HP 14 nm and (right) HP 13 nm. The dashed lines correspond to a constant Z-factor 0.32×10^{-8} and 0.22×10^{-8} mj·nm^3. Shaded areas denote the target specifications of the program. Filled dots correspond to 1:1 ratio of L/S (DtS) for each resist.

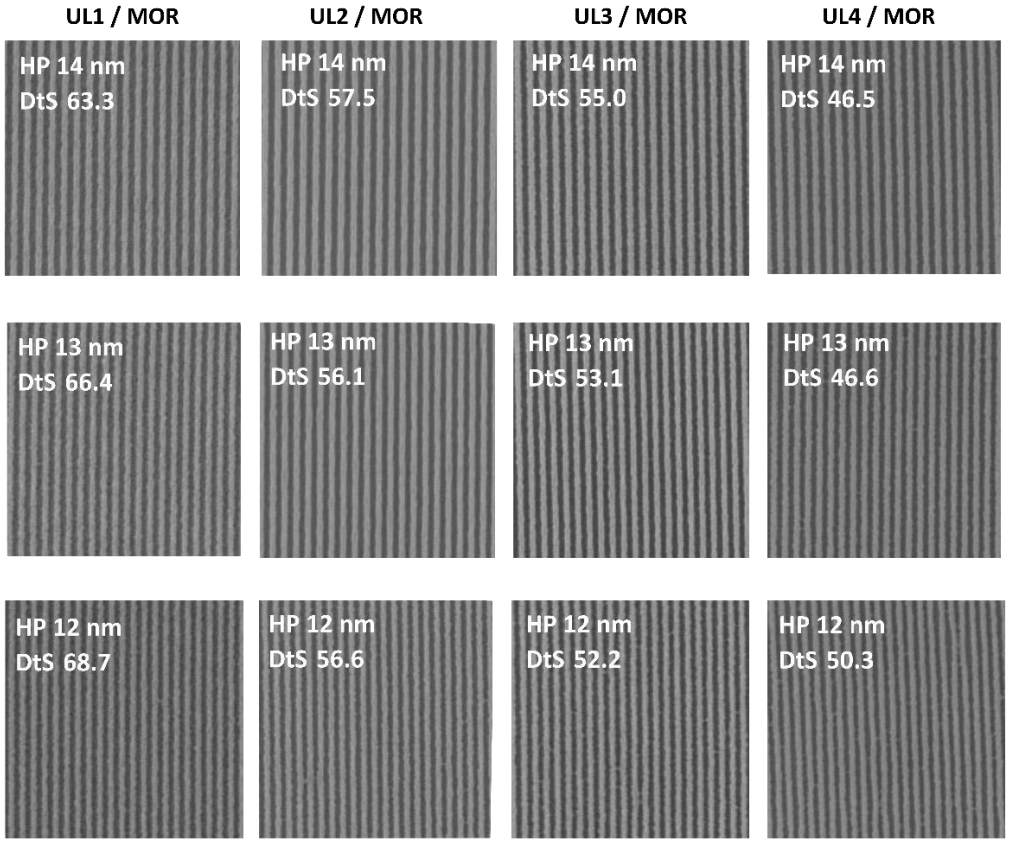

Figure 7. The performance of the same MOR with different UL for HP 14, 13, and 12 nm.

As already mentioned before, specifically for the MOR resist we performed an evaluation of different underlayers (UL) to see their effect on the resist behavior. Figure 7 shows the performance of the same MOR shown in Figure 5 with different underlayers for HP 14, 13, and 12 nm. DtS decreases from 63.3 mJ/cm^2 (UL1) to 46.5 mJ/cm^2 (UL4) for HP 14 nm, from 66.4 mJ/cm^2 (UL1) to 46.6 mJ/cm^2 (UL4) for HP 13 nm and from 68.7 mJ/cm^2 (UL1) to 50.3 mJ/cm^2 (UL4) for HP 12 nm. There is a significant improvement in DtS of 26% from worst to best performing underlayer. ULs do not only impact the resist performance by promoting adhesion and preventing pattern collapse but can also play a very important role during exposure, post-exposure bake, or development and impact the DtS.

Figure 8 shows the advancements in MOR in 2023 for HP 14 and 13 nm compared to earlier results in 2022. The MOR used to test ULs in 2022 shows a lower DtS but much higher LWR and therefore higher Z-factor, while the MOR in 2023 has a higher DtS but much lower LWR and consequently a lower Z-factor. The delay between exposure and the post-exposure bake/development stage has a lesser impact on the quality of lines in the new MOR compared to the one used in 2022.[14]

To demonstrate the progress in resist development over time, we calculate the Z-factor for the best resists, CAR, MOR, and MTR that were evaluated in this program and plot their evolution over time for the past 3.5 years. The results are shown in Figure 9. For the best resist in each category, we show the corresponding SEM image. The results show a clear trend towards lower Z-factors that shows an improvement in resist performance in all three types of resists. In 2023, CAR and MTR have reached the lowest Z-factor value to date with 0.22.

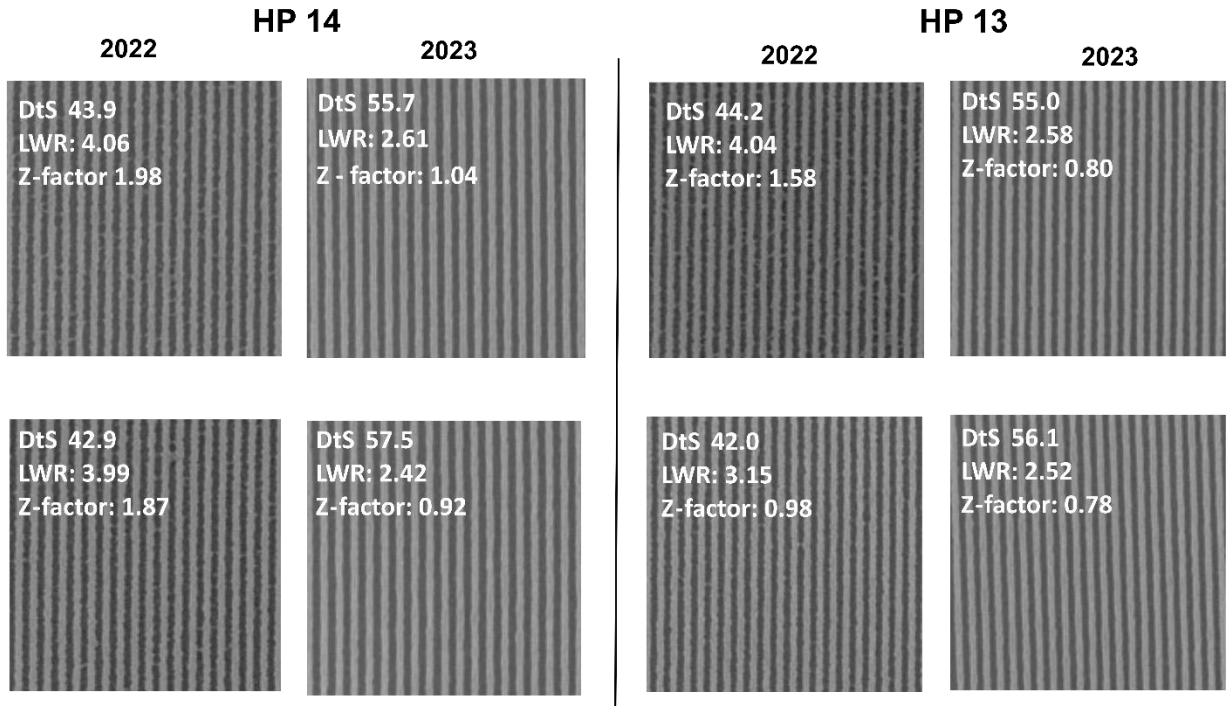

Figure 8. Advancements in MOR in 2023 for HP 14 and 13 nm. The new MOR in 2023 has higher DtS but lower roughness and Z-factor compared to the MOR in 2022.

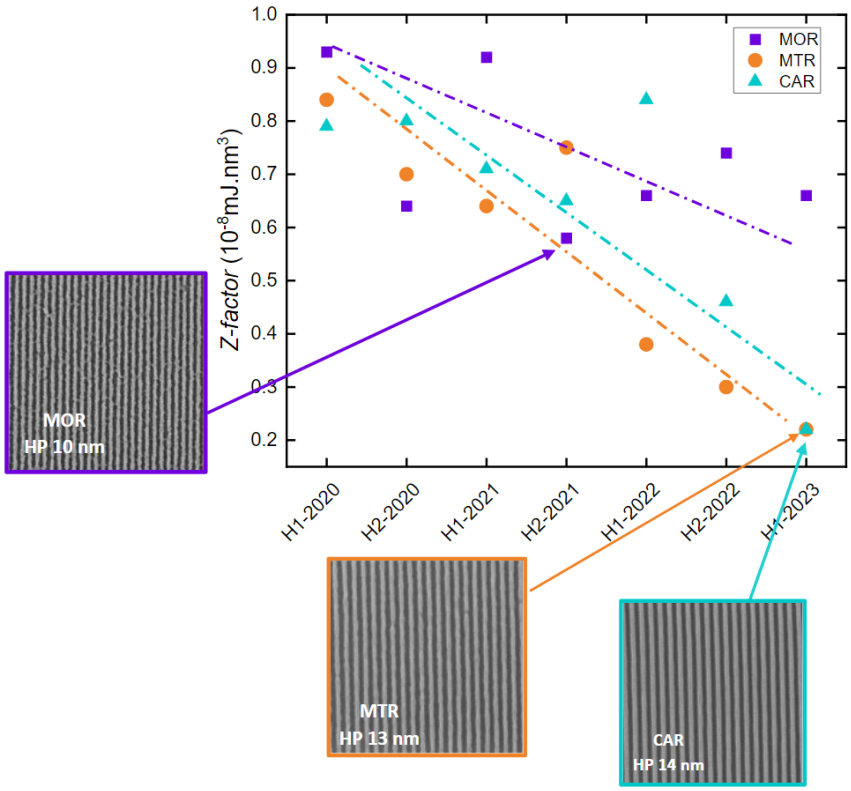

Figure 9. Z-factor evaluation of the best performing CAR, MTR and MOR over the past 3.5 years and SEM images of the resists with the lowest Z-factor for each category. CAR and MTR have the lowest Z-factor to date with 0.22.

CONCLUSIONS

In this paper, we presented an update on the resist screening program carried out at PSI in collaboration with ASML. In 2023, we characterized more than 100 photoresists from six different vendors. We presented results of 14 nm resolution and beyond for three CARs, one MTR, and one MOR with resolutions from HP 14 to 10 nm. We also investigated the effect of different ULs on a particular MOR. CARs provided from two vendors have a resolution down to HP 11 nm, while MTR has a resolution limit at HP 13 nm. However, the MTR shows better performance in terms of DtS and Z-factor. We also demonstrated that the UL plays a significant role during the exposure and development and has a noticeable effect on the performance of MORs. There is also a significant improvement in MOR resist in 2023 in terms of LWR and Z-factor compared to 2022. The general progress in Z-factor over the last 3.5 years shows that the overall performance of all three types of resists has been improving. CAR and MTR have reached the lowest Z-factor to date. This trend shows on one hand that most likely the resists will reach the strict high-NA targets on time and on the other hand stresses the necessity for stronger academic and industrial collaborations in the field of resist development and evaluation.

REFERENCES

1. Van Es, R., van de Kerkhof, M., Minnaert, A., Fisser, G., do Klerk, J., et al, “EUV for HVM: towards an industrialized scanner for HVM NXE3400B performance update.” Proc. SPIE, Extreme Ultraviolet (EUV) Lithography IX, 10583, 105830H, 2018.

2. Wang, X., Tasdemir, Z., Mochi, I., Vockenhuber, M., van Lent-Protasova, L., Meeuwissen, M., Custers, R., Rispens, G., Hoefnagels, R., Ekinci, Y. “Progress in EUV resists towards high-NA EUV lithography.” Proc. SPIE, Extreme Ultraviolet (EUV) Lithography X, 10957, 109570A, 2019.

3. Van Schoot, J., van Setten, E., Troost, K., Lok, S., Stoeldraijer, J., Peeters, R., Benschop, J., Zimmerman, J., Graeupner, P., Wischmeier, L., Kuerz, P. “High-NA EUV lithography exposure tool: program progress.” Proc. SPIE, Extreme Ultraviolet (EUV) Lithography XI, 11323, 1132307, 2020.

4. Allenet, T., Vockenhuber, M., Yeh C.K., Garcia-Santaclara J., van Lent-Protasova L., Ekinci Y., Kazazis D. “EUV resist screening update: progress towards high-NA lithography.” Proc. SPIE, Advances in Patterning Materials and Processes XXXIX, 12055, 120550F 2022.

5. Lorusso, G.F., Sutani, T., Rutigliani, V., Van Roey, F., Moussa, A., Charley, A.L., Mack, C., Naulleau, P., Perera, C., Constantoudis, V. and Ikota, M. “Need for LWR metrology standardization: the imec roughness protocol.” Journal of Micro/Nanolithography, MEMS, and MOEMS, 17(4), 041009, 2018.

6. Mochi, I., Vockenhuber, M., Allenet, T., Ekinci, Y. “Contacts and lines SEM image metrology with SMILE”. Proc. SPIE, Photomask Technology, 11855, 1185502, 2021.

7. Mojarad N., Gobrecht J., Ekinci Y. “Interference lithography at EUV and soft X-ray wavelengths: Principles, methods, and applications,” Microelectronic Engineering.,143, 55-63, 2015.

8. Wang X., Kazazis D., Tseng L.T., Robinson AP., Ekinci Y. “High-efficiency diffraction gratings for EUV and soft x-rays using spin-on-carbon underlayers.” Nanotechnology. 33(6), 065301, 2021.

9. Fallica, R., Kirchner, R., Ekinci, Y., Mailly, D. “Comparative study of resists and lithographic tools using the Lumped Parameter Model.” Journal of Vacuum Science & Technology B, 34(6), 06K702, 2016.

10. Langner A, Solak H.H, Gronheid R, van Setten E, Auzelyte V, Ekinci Y, van Ingen Schenau K, Feenstra K., “Measuring resist-induced contrast loss using EUV interference lithography.” Proc. SPIE, Extreme Ultraviolet (EUV) Lithography, 7636, 76362X, 2010.

11. Sanchez, M.I., Hinsberg, W.D., Houle, F.A., Hoffnagle, J.A., Ito, H. and Nguyen, C.V., “Aerial image contrast using interferometric lithography: effect on line-edge roughness.” Proc. SPIE, Advances in Resist Technology and Processing XVI, 3678, 160, 1999.

12. Fan D., Ekinci Y. “Photolithography reaches 6 nm half-pitch using EUV light.” Journal of Micro/Nanolithography, MEMS, and MOEMS, 15(3), 033505-033505, 2016.

13.Wallow, T., Higgins, C., Brainard, R., Petrillo, K., Montgomery, W., Koay, C.S., Denbeaux, G., Wood, O., Wei, Y. “Evaluation of EUV resist materials for use at the 32 nm half-pitch node.” Proc. SPIE, Emerging Lithographic Technologies XII, 6921, 69211F, 2008.

14. Develioglu, A., Allenet, T.P., Vockenhuber, M., van Lent-Protasova, L., Mochi, I., Ekinci, Y. and Kazazis, D., “The EUV lithography resist screening activities in H2-2022”, Proc. SPIE, Advances in Patterning Materials and Processes XL, 12498, 1249805, 2023.